EARTHQUAKE ENGINEERING AND STRUCTURAL DYNAMICS, VOL. 25, 195–215 (1996)

AN ITERATIVE SOLUTION METHOD FOR DYNAMIC RESPONSE OF BRIDGE–VEHICLES SYSTEMS

FUHENG YANG* AND GHISLAIN A. FONDER†

MSM Department, Institute of Civil Engineering, University of Liège, Quai Banning, 6, 4000, Liège, Belgium

SUMMARY

An iterative solution method is presented and illustrated to analyse the dynamic response of bridge–vehicle systems. The method consists in dividing the whole system into 2 subsystems at the interface of the bridge and vehicles; these 2 subsystems are solved separately; their compatibility at the interface is achieved by an iterative procedure with under-relaxation or with Aitken acceleration. The characteristics of this method are explained on a simplified system with 2 degrees of freedom (DOF). The numerical results for a simple example demonstrate the high performances of the proposed method: good convergence rate and high accuracy. Finally, the method is applied to a practical example: the linear dynamic response of the Yangtze-River Bridge at Wuhan under a moving train with 2 locomotives and 4 freight cars. The efficiency is attained because neither formation nor factorisation of the coefficient matrices for the equations of the system are needed at every time step in linear analysis. The Aitken acceleration technique is more efficient in systems with multi-degrees of freedom than the relaxation technique. The proposed method will be even more efficient in non-linear dynamic response because, in this case, the iterations are necessary whether the system is solved as a whole or not.

KEY WORDS: bridge–vehicle interaction; dynamic response; iterative solution

1. INTRODUCTION

The dynamic response of a bridge under moving vehicles has been a very active research subject for a long time. One of the following types of equations is obtained for the system, depending on the method being used:

(1) Coupled equations with an infinite number of DOF for the bridge and a few DOF for the vehicles. They generally result from modelling analytically the bridge as a beam. The system is solved by the infinite series expansion method. Timoshenko and Young[1] used this method and also gave details of early applications.
(2) Coupled equations with a few DOF for both the bridge and the vehicles. They are normally obtained by prescribing the bridge a given shape or combination of given shapes at any time during the passage of the vehicles. Because of the small number of unknowns, the equations for the system can be solved analytically or numerically without difficulty. Wen[2] used this method; Jacobsen and Ayre[3] listed earlier references.
(3) Coupled equations with a large number of DOF for both the bridge and the vehicles. Normally this happens when the bridge is modelled by the finite element method or one of its derivatives like the modal method or the substructure method. The vehicle model can be very complicated. The coupled equations are solved by direct time integration such as the Newmark and Wilson-θ methods. Chu *et al.*[4] gave all the formulas in detail and Wiriyachai *et al.*,[5,6] Nielsen and Abrahamsson[7] used this method.

*Research fellow and formerly, Engineer at Graduate School, China Academy of Railway Sciences, Beijing, People's Republic of China

†Professor of Structural Mechanics

CCC 0098–8847/96/020195–21

Received 24 March 1995
Revised 20 June 1995

(4) Two uncoupled sets of equations, for the bridge and the vehicles, respectively, plus geometrical compatibility conditions and equilibrium conditions for the interaction forces between the bridge and vehicles. The two sets of equations are solved separately and the two sets of limit conditions are satisfied by an iterative procedure. This method was first used by Veletsos and Huang.[8] Since then, it has been used by Xu,[9,10] the first author,[11] Hwang and Nowak,[12] Wang and Huang,[13] Wang *et al.*[14], Huang and Wang,[15] Huang *et al.*[16] and Chatterjee *et al.*[17] This kind of uncoupled sets of differential equations is solved normally by Direct Time Integration methods, namely step-by-step methods. But a new method has been developed recently by Green and Cebon[18] to solve the equations in the frequency domain. They calculate the dynamic response of the bridge by means of the convolution of modal impulse response functions and modal exciting forces, together with the modal superposition; these convolutions are computed with the FFT and IFFT methods.

Although much attention has been paid to the solution of these uncoupled equations, the problem is not yet satisfactorily solved.

The first two methods are applicable only when the bridge has a shape simple enough so that credible deformation modes can be guessed; they are rarely used anymore. Nowadays, sophisticated models are deemed necessary for the bridge and the vehicles; for example, girder bridges, suspension bridges and cable-stayed bridges require many DOF; a single freight train car requires 27 DOF in Xu's papers.[9,10] Hence the success of the last two methods about which the following comments can be made.

The method of coupled equations for the system is not convenient because of the following difficulties:

(a) The coefficient matrices of equations for the system vary according to the position of the vehicles on the bridge and therefore the matrices must be updated and factorized at every time step.
(b) The formulation and hence the programming for the coefficient matrices depend on both the bridge and vehicle models: if a new type of car or a new type of bridge is introduced, all coefficients must be changed. Furthermore, they are complicated to establish and much computational effort must be devoted to obtain them.
(c) The more vehicles on the bridge, the more coupled DOF and also the more DOF in the coupled equations for the system.
(d) The more coupled DOF, the less sparse the coefficient matrices.

All these inconveniences render the coupled equations very difficult to solve in view of either memory allocation or computational effort.

Therefore, some researchers attempt to avoid coupled equations for the system by assuming a fixed deformed shape for the bridge deck to study the characterisitcs of the vehicles crossing it (Keymeulen and Winand[19]) or by replacing the vehicles with a supposed train load–time distribution to calculate the dynamic response of the bridge (Van Bogaert[20], and Saadeghvaziri[21]). Xu[10] showed that the wheel–rail interaction forces when a train is travelling on the bridge are very different from those on the normal track and the bridge–vehicle system must be solved as a whole.

For uncoupled sets of equations, various iterative solution methods were used. In Veletsos and Huang's method[8], one interaction solution of the bridge and the vehicles is needed for solving every degree of freedom of the bridge or the vehicles within one iteration. This complicates the implementation of the bridge–vehicles interaction. Hwang and Nowak's method[14] is similar to the Jacobi iteration, in which the improvement of the unknowns both from the bridge and vehicles is based on their values at the previous iteration stage. The method used by Wang and Huang,[13] Wang *et al.*,[14] Huang and Wang[15] and Huang *et al.*[16] is really a block Gauss–Seidel iteration; only two blocks are presented and the solution for the unknowns related to the vehicles depends on the assumption for the unknowns related to the bridge; this means that only the assumption for the unknowns related to the bridge needs to be made. Green and Cebon's iteration method[13] is similar to the one proposed in this paper but with the specific relaxation coefficient $\eta = 0{\cdot}5$.

Nevertheless, there is little or no information about the convergence characteristics of the existing iterative solution methods; furthermore, few details about the iteration schemes are made available to readers except

by Veletsos and Huang, and Green and Cebon. Green and Cebon's iteration method can be extended with the relaxation concept proposed in this paper and a better convergence rate should be obtained if a good relaxation coefficient is used. The objective of this paper is to present in detail an iterative method with relaxation or with Aitken acceleration to solve separately the equations of motion for the bridge and vehicles and to provide some knowledge about its convergence characteristics. The method is first applied to a simple example and then to a practical one, namely the dynamic response of the Yangtze-River Bridge at Wuhan under a moving train with 2 locomotives and 4 freight cars. Although the Newmark method has been chosen, the proposed concept is applicable to equations integrated by other direct time-integration methods.

2. ALGORITHM OF THE PROPOSED METHOD

The idea is that, during the passage of the vehicles across a bridge, on the one hand, the vehicles excite the bridge only by their interaction forces, and, on the other hand, the bridge excites the vehicles only by its own movement. To present clearly the proposed method, most symbols are illustrated in a typical bridge–vehicle system (vehicles can be any model and the bridge–vehicles interface can be any) shown in Figure 1 and all the necessary equations are listed below.

The equation of motion for the bridge and vehicles are:

$$M_b\ddot{X}_b + C_b\dot{X}_b + K_bX_b = P_b \tag{1}$$

$$M_v\ddot{X}_v + C_v\dot{X}_v + K_vX_v = P_v \tag{2}$$

$$P_b = F_{bg} + F_b \tag{3}$$

$$P_v = F_{vg} + F_v \tag{4}$$

$$F_b = F_b(\ddot{X}_v, \dot{X}_v, X_v, \ddot{X}_b, \dot{X}_b, X_b) \tag{5}$$

$$F_v = F_v(\ddot{X}_b, \dot{X}_b, X_b) \tag{6}$$

where X_b/X_v are the DOF associated with the bridge/vehicles, respectively, M_b/M_v, C_b/C_v, K_b/K_v are the mass, damping and stiffness matrices for the bridge/vehicles, P_b/P_v are the total external forces for the bridge/vehicles, F_{bg}/F_{vg} are the forces acting on the bridge/vehicles which are independent of the bridge and vehicle movement (gravity force for example), F_b/F_v are the movement dependent forces acting on the bridge/vehicles; by hypothesis, the former depends on the bridge and vehicles movement while the latter depends only on the bridge movement.

The geometrical compatibility imposes the equality of the displacements at the contact points between the bridge and vehicles:

$$X_v^i = X_b^i + Y_s \quad \text{at any instant} \tag{7}$$

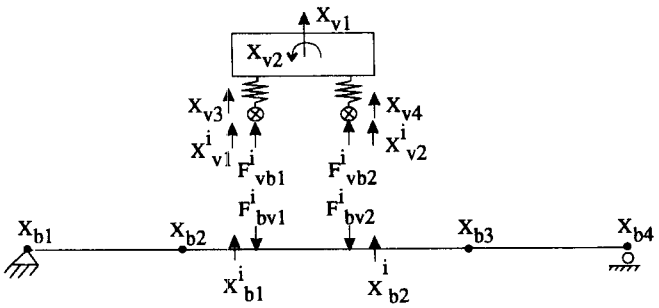

Figure 1. Typical bridge–vehicle system

where the superscript i indicates an interface point, which usually does not coincide with a DOF, Y_s is the additional disturbance due to the irregularities of railway tracks or the roughness of the road surface.

The equilibrium imposes the equality of the interaction forces at the same contact points:

$$F^{i}_{bv} = F^{i}_{vb} \quad \text{at any instant} \tag{8}$$

where F^{i}_{vb} is the force onto the vehicles from the bridge, and F^{i}_{bv} is the force onto the bridge from the vehicles, they must be converted later to statically equivalent nodal forces associated with DOF or general DOF. The force F^{i}_{vb} can be calculated from the motion of vehicles by means of:

$$F^{i}_{vb} = F^{i}_{vb}(\ddot{X}_v, \dot{X}_v, X_v, F_{vg}, \ddot{X}_b, \dot{X}_b, X_b) \tag{9}$$

The motion of the whole system is governed by these 9 equations. If the Newmark method is used to integrate the equations of motion from time t_0 to time $t = t_0 + \Delta t$, the following expressions are obtained:

$$^{t}\dot{X}_b = a_2(^{t}X_b - {}^{0}X_b) - a_5{}^{0}\dot{X}_b - a_6{}^{0}\ddot{X}_b \tag{10}$$

$$^{t}\ddot{X}_b = a_1(^{t}X_b - {}^{0}X_b) - a_3{}^{0}\dot{X}_b - a_4{}^{0}\ddot{X}_b \tag{11}$$

$$^{t}\dot{X}_v = a_2(^{t}X_v - {}^{0}X_v) - a_5{}^{0}\dot{X}_v - a_6{}^{0}\ddot{X}_v \tag{12}$$

$$^{t}\ddot{X}_v = a_1(^{t}X_v - {}^{0}X_v) - a_3{}^{0}\dot{X}_v - a_4{}^{0}\ddot{X}_v \tag{13}$$

where

$$a_1 = \frac{1}{\alpha\Delta t^2}, \qquad a_2 = \frac{\delta}{\alpha\Delta t}, \qquad a_3 = \frac{1}{\alpha\Delta t}$$

$$a_4 = \frac{1}{2\alpha} - 1, \qquad a_5 = \frac{\delta}{\alpha} - 1, \qquad a_6 = \left(\frac{\delta}{2\alpha} - 1\right)\Delta t$$

and α, δ are Newmark parameters, for example $\alpha = 0{\cdot}25$, $\delta = 0{\cdot}5$ corresponding to the Average Acceleration Method. The left superscript ${}^{0}\{\ \}$ and ${}^{t}\{\ \}$ indicate instant t_0 and t, respectively.

The equations of motion, i.e. equations (1) and (2), can be written at instant t:

$$(K_b + a_1M_b + a_2C_b)^{t}X_b = {}^{t}P_b + M_b(a_1{}^{0}X_b + a_3{}^{0}\dot{X}_b + a_4{}^{0}\ddot{X}_b) + C_b(a_2{}^{0}X_b + a_5{}^{0}\dot{X}_b + a_6{}^{0}\ddot{X}_b) \tag{14}$$

$$(K_v + a_1M_v + a_2C_v)^{t}X_v = {}^{t}P_v + M_v(a_1{}^{0}X_v + a_3{}^{0}\dot{X}_v + a_4{}^{0}\ddot{X}_v) + C_v(a_2{}^{0}X_v + a_5{}^{0}\dot{X}_v + a_6{}^{0}\ddot{X}_v) \tag{15}$$

After time integration, the motion of the whole system is controlled by equations (3)–(15): the displacements ${}^{t}X_b$ and ${}^{t}X_v$ at instant t are the primary unknowns; the velocities and acceleration can be found from equations (10)–(13). The following algorithm of iterative procedure is proposed to solve for these two subsets of displacements.

Iterative algorithm

1. Start a Newmark time step. All variables are known at $t = t_0$, including
$$^{0}\ddot{X}_b, {}^{0}\dot{X}_b, {}^{0}X_b \quad \text{and} \quad {}^{0}\ddot{X}_v, {}^{0}\dot{X}_v, {}^{0}X_v$$
2. Initialize for the Newmark time step.
   (a) $t = t_0 + \Delta t$ and determine if the Newmark time step terminates.
   (b) Compute the movement independent variables at instant t:
$$^{t}F_{bg}, \qquad ^{t}F_{vg}$$
   Note that ${}^{t}F_{bg}$ should include the movement independent forces (gravity for instance) applied either directly to the bridge or to the vehicles and then indirectly to the bridge via the interaction forces. To simplify the procedure, the latter part is computed at Step 7 together with the

movement-dependent interaction forces. This treatment does not increase much the computation effort and is acceptable in practice in view of simplicity.

(c) Compute the quantities dependent on the variables evaluated at instant t_0:

$$S_b = M_b({a_1}^0 X_b + {a_3}^0 \dot{X}_b + {a_4}^0 \ddot{X}_b) + C_b({a_2}^0 X_b + {a_5}^0 \dot{X}_b + {a_6}^0 \ddot{X}_b)$$

$$S_v = M_v({a_1}^0 X_v + {a_3}^0 \dot{X}_v + {a_4}^0 \ddot{X}_v) + C_v({a_2}^0 X_v + {a_5}^0 \dot{X}_v + {a_6}^0 \ddot{X}_v)$$

These quantities will be used in equations (14) and (15).

3. Initialize for iterations within one Newmark time step.
   (a) Take the last known value at instant t_0 as the initial guess for the motion of the bridge at instant t:

$$^t X_b^{(0)} = {}^0 X_b$$

   where the right superscript $\{\}^{(0)}$ indicates the start value of iteration.
   (b) Initialize the counter of the iteration number: $k = 0$.
4. Calculate the velocity and acceleration of the bridge at time t from equations (10) and (11).
5. Compute the excitation of the vehicles, i.e. the movement of the vehicles at the contact points due to the movement of the bridge, from the geometrical compatibility equation (7).
6. Solve for the motion of vehicles at instant t.
   (a) Compute the excitation forces on the vehicles which are dependent on the motion of the bridge from equation (6); the excitation coming from the irregularities of railway tracks or the roughness of the road surface (i.e. additional excitation from the bridge–vehicle interface, for example see Figure 3), which is independent of the bridge motion, can be eventually added at this level.
   (b) Compute the total forces (movement dependent and movement independent) from equation (4).
   (c) Compute the displacement of vehicles from equation (15).
   (d) Compute the velocity and acceleration of vehicles from equations (12) and (13).
7. Compute the forces associated with the bridge DOF from the interaction forces. (Here all the forces coming from the vehicles, including the movement-dependent and movement-independent parts are applied together.)
   (a) Compute the forces F^i_{vb} on the vehicles at contact points from equation (9).
   (b) Compute the forces F^i_{bv} on the bridge from the equilibrium of interaction forces, equation (8).
   (c) Compute the forces associated with the bridge DOF due to F^i_{bv} by means of equation (5).
   (d) Compute the total forces [movement-independent and movement-dependent parts, i.e. the part obtained at Step 2(b) and that at Step 7(c)] associated with the bridge DOF by means of equation (3).
8. Solve equation (14) to find $^t X_b$ which is a trial value for the motion of the bridge to be compared with the last available guess $^t X_b^{(k)}$ during the kth iteration.
9. Check convergence.
   (a) Compute the difference and its norm:

$$\Delta X_b^{(k)} = {}^t X_b - {}^t X_b^{(k)}$$

$$\text{Norm}(\Delta X_b^{(k)}) = \sum_{i=1}^{n} (\Delta X_b^{(k)}(i))^2$$

   where n is the number of degrees of freedom of the bridge and $\Delta X_b^{(k)}(i)$ is the ith component of the vector $\Delta X_b^{(k)}$.
   (b) Compare with a convergence criterion

$$\frac{\text{Norm}(\Delta X_b^{(k)})}{\text{Norm}(\Delta X_b^{(0)})} \leqslant \varepsilon$$

where ε is assumed between $1{\cdot}0 \times 10^{-5}$ and $1{\cdot}0 \times 10^{-8}$, usually sufficient to obtain the solution with reasonable accuracy.

10. Decide whether the next iteration or the next Newmark time step is to be effected.
    (a) If convergence is not achieved, an improved trial value for the motion of the bridge which is based on the guess ${}^{t}X_{b}^{(k)}$ can be obtained either by relaxation or Aitken acceleration.

Relaxation: If the relaxation technique is used, the relaxation procedure is effected for every iterative step:

$$ {}^{t}X_{b}^{(k+1)} = {}^{t}X_{b}^{(k)} + \eta \Delta X_{b}^{(k)} $$

where η is a relaxation coefficient. It must be in a certain range $(0 < \eta < \eta_{max})$ to ensure convergence of the iterations; η_{max} is the upper bound of the relaxation coefficient; it will be demonstrated that $\eta_{max} < 2$ and that $\eta = 0{\cdot}5\eta_{max}$ is the optimal relaxation coefficient. The above improved result is a new guess for the next iteration. Then go to Step 11.

Aitken acceleration: If the Aitken acceleration[22] is used, the starting value for the next iteration is determined as follows:

If k is even, or saying it is an even iteration, then let

$$ {}^{t}X_{b}^{(k+1)} = {}^{t}X_{b} $$

and compute the difference

$$ \Delta_1 = {}^{t}X_{b}^{(k+1)} - {}^{t}X_{b}^{(k)} $$

then go to Step 11;

If it is an odd iteration, the Aitken acceleration procedure should be effected: compute

$$ \Delta_2 = {}^{t}X_{b} - {}^{t}X_{b}^{(k)} $$

and effect the acceleration procedure

$$ {}^{t}X_{b}^{(k+1)}(i) = {}^{t}X_{b}^{(k)}(i) + \frac{\Delta_1(i)\Delta_2(i)}{\Delta_1(i) - \Delta_2(i)}, \quad (i = 1, 2, \ldots, n) $$

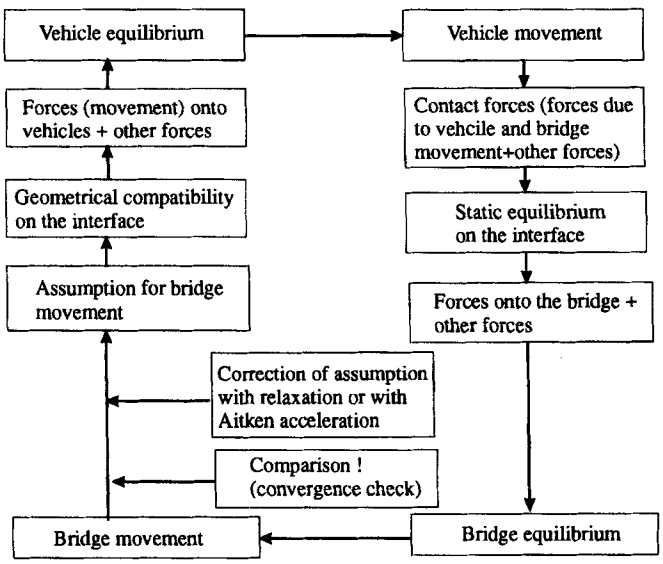

Figure 2. Iterative solution scheme

then go to Step 11. Noting that the Aitken acceleration procedure is effected every two iterative steps.

(b) If convergence is achieved, compute the velocity and acceleration of the bridge by means of equations (10) and (11) and proceed to the next instant. Hence return to Step 1 for the next Newmark time step.

11. Pass to the next iteration. Increase the iteration counter k by one:

$$k \Leftarrow k + 1$$

and return to Step 4 for the next iteration.

The above algorithm seems complicated, so a helpful diagram presentation is made in Figure 2.

3. CHARACTERISTICS OF THE PROPOSED ALGORITHM FOR A SIMPLIFIED SYSTEM

A 2 DOF system, which is simple enough to be solved analytically, is considered to examine the characteristics of the proposed method (Figure 3). In this example, the mass m_1 acts as the bridge and m_2 the vehicles. This example is different from a bridge under moving vehicles in that point: m_2 does not move. Nevertheless, to examine the convergence characteristics of an iterative solution for given individual time steps, there is no difference between the two systems. $\alpha = 0{\cdot}25$ and $\delta = 0{\cdot}5$ are used for the parameters of the Newmark method. To apply the proposed method, this system must be separated into two sprung masses acting as the bridge and vehicles, respectively. Thus the equations of motion are:

$$m_1\ddot{x}_1 + c_1\dot{x}_1 + k_1x_1 = {}^tp_1 + f_{12} \tag{16}$$

$$m_2\ddot{x}_2 + c_2\dot{x}_2 + k_2x_2 = {}^tp_2 + c_2\dot{x}_1 + k_2x_1 \tag{17}$$

with $c_1 = 2\xi_1\sqrt{m_1k_1}$, $c_2 = 2\xi_2\sqrt{m_2k_2}$ and $f_{12} = c_2(\dot{x}_2 - \dot{x}_1) + k_2(x_2 - x_1)$, which is the interaction force.

If equations (16) and (17) are compared with equations (1)–(6), it can be observed that equations (7)–(9) are used directly in establishing these two equations because of the simplicity of this example, and :

$$F_{bg} = {}^tp_1, \qquad F_{vg} = {}^tp_2$$

$$F_b = c_2(\dot{x}_2 - \dot{x}_1) + k_2(x_2 - x_1), \qquad F_v = c_2\dot{x}_1 + k_2x_1$$

The following values are used to obtain the numerical results:

$$m_1 = 1{\cdot}0, \qquad m_2 = 1{\cdot}0, \qquad k_1 = 1{\cdot}0, \qquad k_2 = 100{\cdot}0$$

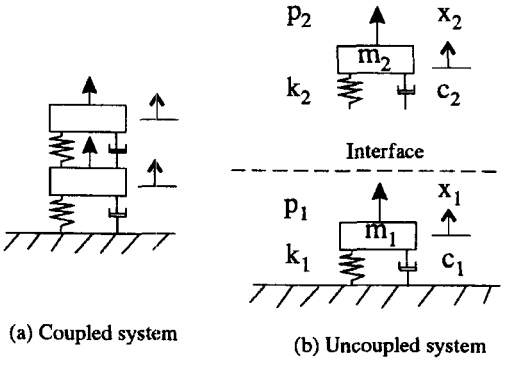

Figure 3. Simplified system

As mentioned in the above section, the convergent value ${}^0x_1$ of displacement x_1 at instant t_0 is taken as the starting value at instant t in the proposed iterative procedure, together with the corresponding velocity [equation (10)]:

$$ {}^t x_1^{(k)} = {}^0x_1, \qquad {}^t\dot{x}_1^{(k)} = \frac{\delta}{\alpha \Delta t}\, {}^t x_1^{(k)} - a_2\, {}^0x_1 - a_5\, {}^0\dot{x}_1 - a_6\, {}^0\ddot{x}_1 $$

where $k = 0$. According to the proposed method, the dynamic response of the mass m_2 could be solved at this point and the corresponding velocity (together with the acceleration if interested) can be computed as follows:

$$ \begin{aligned} {}^t x_2^{(k)} &= \frac{1}{\tilde{k}_2}\left({}^t p_2 + k_2\, {}^t x_1^{(k)} + \frac{c_2 \delta}{\alpha \Delta t}\, {}^t x_1^{(k)} \right) + f_2(t_0) \\ &= \frac{k_2 + d_2}{\tilde{k}_2}\, {}^t x_1^{(k)} + \frac{{}^t p_2}{\tilde{k}_2} + f_2(t_0), \end{aligned} $$

$$ {}^t\dot{x}_2^{(k)} = \frac{\delta}{\alpha \Delta t}\, {}^t x_2^{(k)} - a_2\, {}^0x_2 - a_5\, {}^0\dot{x}_2 - a_6\, {}^0\ddot{x}_2 $$

hence the interaction force between m_1 and m_2 is

$$ f_{12} = c_2({}^t\dot{x}_2^{(k)} - {}^t\dot{x}_1^{(k)}) + k_2({}^t x_2^{(k)} - {}^t x_1^{(k)}) $$

With the above interaction force, the dynamic response of the mass m_1 may be solved during the kth iteration:

$$ \begin{aligned} x_1' &= \frac{1}{\tilde{k}_1}({}^t p_1 + k_2({}^t x_2^{(k)} - {}^t x_1^{(k)}) + c_2({}^t\dot{x}_2^{(k)} - {}^t\dot{x}_1^{(k)})) + f_1(t_0) \\ &= \frac{1}{\tilde{k}_1}\left(\left(k_2 + \frac{c_2 \delta}{\alpha \Delta t} \right)({}^t x_2^{(k)} - {}^t x_1^{(k)}) + {}^t p_1 \right) + f_1(t_0) \\ &= \frac{d_2 + k_2}{\tilde{k}_1}\left(\frac{d_2 + k_2}{\tilde{k}_2}\, {}^t x_1^{(k)} + \frac{{}^t p_2}{\tilde{k}_2} - {}^t x_1^{(k)} \right) + \frac{{}^t p_1}{\tilde{k}_1} + f(t_0) \\ &= -e\, {}^t x_1^{(k)} + \frac{1}{\tilde{k}_1}\left({}^t p_1 + \frac{d_2 + k_2}{\tilde{k}_2}\, {}^t p_2 \right) + f(t_0) \end{aligned} \tag{18} $$

with

$$ e = \frac{k_2 + d_2}{\tilde{k}_1} \cdot \frac{\tilde{k}_2 - k_2 - d_2}{\tilde{k}_2} > 0 $$

In the above formulas, $\tilde{k}_1$, $\tilde{k}_2$, d_1 and d_2 are coefficients given by

$$ \tilde{k}_1 = k_1 + \frac{m_1}{\alpha\, \Delta t^2} + \frac{\delta c_1}{\alpha\, \Delta t}, \quad d_1 = \frac{\delta c_1}{\alpha\, \Delta t} $$

$$ \tilde{k}_2 = k_2 + \frac{m_2}{\alpha\, \Delta t^2} + \frac{\delta c_2}{\alpha\, \Delta t}, \quad d_2 = \frac{\delta c_2}{\alpha\, \Delta t} $$

and $f_1(t_0)$, $f_2(t_0)$ and $f(t_0)$ are functions of the variables evaluated at instant t_0.

Further development for e can be made as follows:

$$e = \frac{1 + d_2/k_2}{m + k + m(d_2/k_2) + k(d_1/k_1) + k/\alpha\,\Delta t^2\omega_1^2 + m\alpha\,\Delta t^2\omega_1^2(1 + d_1/k_1)(1 + d_2/k_2)} \tag{19}$$

$$m = \frac{m_1}{m_2}, \qquad k = \frac{k_1}{k_2}, \qquad \omega_1 = \sqrt{\frac{k_1}{m_1}}$$

The improved starting value of ${}^t x_1$ for the next iteration step $k + 1$ (Relaxation method, every iterative step) or for the iteration step $k + 2$ (Aitken acceleration, every 2 iterative steps) is determined as follows:

Using relaxation technique

If the relaxation technique is used in the proposed procedure, an improved value for the next iteration step is

$$\begin{aligned} {}^t x_1^{(k+1)} &= {}^t x_1^{(k)} + \eta(x_1' - {}^t x_1^{(k)}) \\ &= b\,{}^t x_1^{(k)} + \frac{\eta}{\tilde{k}_1}\left({}^t p_1 + \frac{d_2 + k_2}{\tilde{k}_2}\,{}^t p_2\right) + \eta f(t_0) \end{aligned} \tag{20}$$

with

$$b = 1 - \eta(1 + e) \tag{21}$$

where η is the relaxation coefficient.

Using Aitken acceleration

If the Aitken acceleration is used, the acceleration will be effected for every two iteration steps, i.e. the starting value for the next iteration step $k + 1$ is simply taken as

$${}^t x_1^{(k+1)} = x_1' = -e\,{}^t x_1^{(k)} + \frac{1}{\tilde{k}_1}\left({}^t p_1 + \frac{d_2 + k_2}{\tilde{k}_2}\,{}^t p_2\right) + f(t_0)$$

and the further iteration step [equation (18)] gives

$$\begin{aligned} x_1' &= -e\,{}^t x_1^{(k+1)} + \frac{1}{\tilde{k}_1}\left({}^t p_1 + \frac{d_2 + k_2}{\tilde{k}_2}\,{}^t p_2\right) + f(t_0) \\ &= e^2\,{}^t x_1^{(k)} + (1 - e)\frac{1}{\tilde{k}_1}\left({}^t p_1 + \frac{d_2 + k_2}{\tilde{k}_2}\,{}^t p_2\right) + (1 - e) f(t_0) \end{aligned}$$

Noting that

$$\Delta_1 = {}^t x_1^{(k+1)} - {}^t x_1^{(k)}$$

$$\begin{aligned} \Delta_2 = x_1' - {}^t x_1^{(k+1)} &= -(1 + e)\,{}^t x_1^{(k+1)} + \frac{1}{\tilde{k}_1}\left({}^t p_1 + \frac{d_2 + k_2}{\tilde{k}_2}\,{}^t p_2\right) + f(t_0) \\ &= (1 + e)e\,{}^t x_1^{(k)} + (-1 - e + 1)\left(\frac{1}{\tilde{k}_1}\left({}^t p_1 + \frac{d_2 + k_2}{\tilde{k}_2}\,{}^t p_2\right) + f(t_0)\right) \\ &= e\left(e\,{}^t x_1^{(k)} - \frac{1}{\tilde{k}_1}\left({}^t p_1 + \frac{d_2 + k_2}{\tilde{k}_2}\,{}^t p_2\right) - f(t_0) + {}^t x_1^{(k)}\right) \\ &= e(-\Delta_1) \end{aligned}$$

according to the formula of the Aitken acceleration, the final improved value for the starting value at the iterative step $k+2$ is

$$
\begin{aligned}
{}^{t}x_1^{(k+2)} &= {}^{t}x_1^{(k+1)} + \frac{\Delta_1 \Delta_2}{\Delta_1 - \Delta_2} \\
&= {}^{t}x_1^{(k+1)} - \frac{e}{1+e}\Delta_1 \\
&= \frac{1}{1+e}\,{}^{t}x_1^{(k+1)} + \frac{e}{1+e}\,{}^{t}x_1^{(k)} \\
&= \frac{1}{1+e}\left(-e\,{}^{t}x_1^{(k)} + \frac{1}{\tilde{k}_1}\left({}^{t}p_1 + \frac{d_2+k_2}{\tilde{k}_2}\,{}^{t}p_2\right) + f(t_0) + e\,{}^{t}x_1^{(k)}\right) \\
&= \frac{1}{1+e}\left(\frac{1}{\tilde{k}_1}\left({}^{t}p_1 + \frac{d_2+k_2}{\tilde{k}_2}\,{}^{t}p_2\right) + f(t_0)\right)
\end{aligned}
\tag{22}
$$

Convergence characteristics if using relaxation technique

From equation (20), the usual stability criterion (spectral radius of the operator matrix not greater than one) indicates that the iterative procedure is convergent *if and only if*

$$-1 < b < 1 \tag{23}$$

From this equation and equation (21), the bound for the relaxation coefficient can be derived as follows:

$$0 < \eta < \eta_{\max} \quad \text{but } \eta_{\max} < 2 \tag{24}$$

where

$$\eta_{\max} = \frac{2}{1+e} \tag{25}$$

From equations (19) and (25), it can be observed that:

(1) The exact value of the upper bound of the relaxation coefficient is a function of damping, $\omega_1 \Delta t$ and the mass and stiffness ratios (m, k);
(2) The damping ξ_1 on m_1 increases $\eta_{\max}$ slightly, but the damping ξ_2 on m_2 (on the interface of the two subsystems) decreases $\eta_{\max}$. Figures 4 and 5 show, respectively, the $\eta_{\max}$ versus ξ_1 and ξ_2 relations in the case where parameter $\Delta t = 0{\cdot}15 \approx \frac{1}{4}T_2$ (natural period of the mass m_2) is chosen.

From these figures, it is observed that damping has little influence on $\eta_{\max}$. Hence $\eta_{\max}$ can be estimated by ignoring damping. Introducing

$$e \approx e_0 = \frac{1}{m + k + (k/\alpha \Delta t^2 \omega_1^2) + m\alpha \Delta t^2 \omega_1^2} \leqslant \frac{1}{(\sqrt{m} + \sqrt{k})^2} \tag{26}$$

$\eta_{\max}$ can be approximated as follows:

$$\eta_{\max} \approx \frac{2}{1+e_0} \geqslant \frac{2}{1 + 1/[(\sqrt{m} + \sqrt{k})^2]} \tag{27}$$

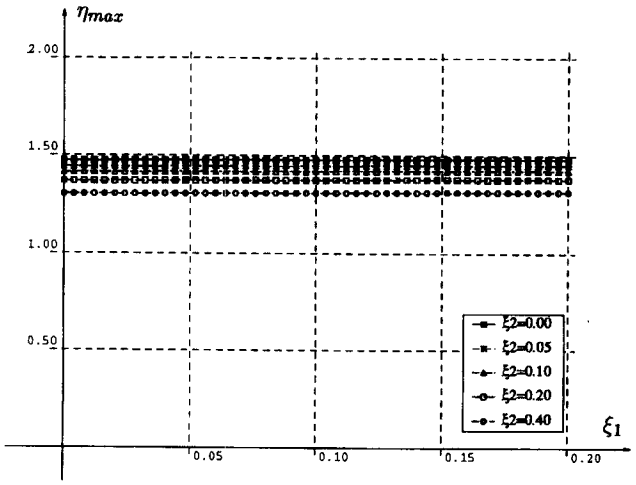

Figure 4. Influence of damping ξ_1 on the upper bound η_{max} of the relaxation coefficient

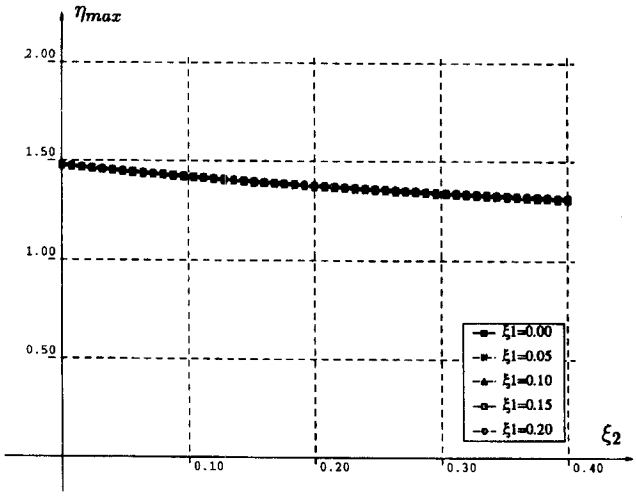

Figure 5. Influence of damping ξ_2 on the upper bound η_{max} of the relaxation coefficient

Equation (27) gives an estimate for the minimum value of the upper bound on the relaxation coefficient. The value of $\omega_1 \Delta t$ significantly influences η_{max}. Figure 6 shows the η_{max} versus $\omega_1 \Delta t$ relation without damping. In this figure, the minimum value (dash line) is computed by means of equation (27). Figure 7 gives the curves of the minimum of η_{max} versus k for different values of m [equation (27)]. This is very useful to estimate the range of the relaxation coefficient for the simplified system.

From equation (20), another interesting conclusion can be found: the iterative procedure has the best convergence rate if $b = 0$. In this case, the relaxation coefficient should be equal to the best relaxation coefficient, which is evaluated as

$$\eta_{optimum} = \tfrac{1}{2}\eta_{max} = \frac{1}{1+e} < 1 \tag{28}$$

Equation (28) shows that the best relaxation coefficient is always lower than unity. This means that under-relaxation is necessary for the kind of iteration proposed in this paper. If a relaxation coefficient close

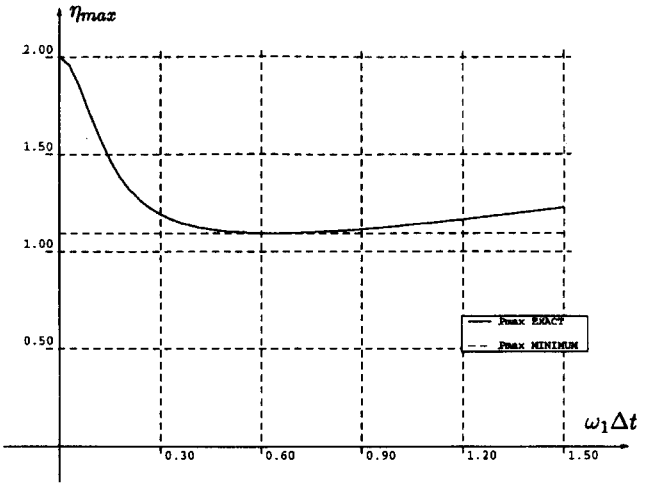

Figure 6. Influence of $\omega_1 \Delta t$ on the upper bound η_{max} of the relaxation coefficient

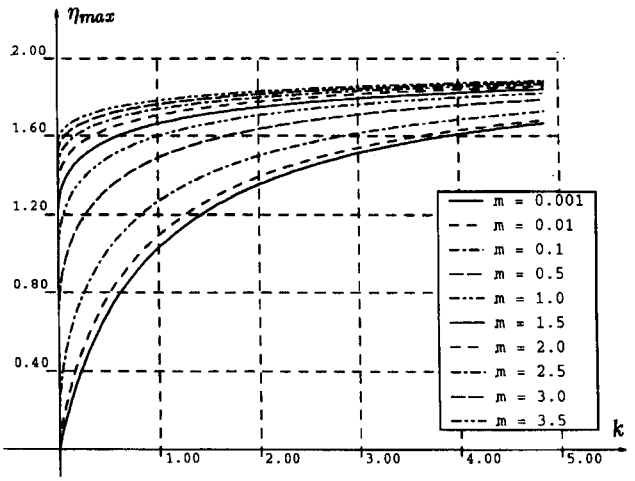

Figure 7. Minimum of the upper bound η_{max} of the relaxation coefficient versus k

to the best one is used, the convergence rate will be good. Equations (24), (27) and (28) give an estimate of the range and the best value of the relaxation coefficient for the proposed algorithm in the previous section when relaxation is used.

Convergence characteristics if using Aitken acceleration

Equation (22) tells that the iterative coefficient

$$b = 0$$

i.e. within one Aitken acceleration step (saying within two simple iterative steps), the iterative procedure will find its exact solution if the system is linear. This convergence behaviour is well appreciated. In case using relaxation, $b = 0$ is true only if the best relaxation coefficient is used; otherwise, b is not zero. But it is not needed to find the best relaxation coefficient if Aitken acceleration is used and a good convergence rate will be still obtained. The performance of the Aitken acceleration will be demonstrated with the second example in the next section.

These formulas are derived from the simple 2 DOF system, but they are applicable to complicated systems if they can be simplified to the system shown in Figure 3. An experienced engineer knows how to establish a simple model for the bridge–vehicles systems when the vehicles are at specific positions on the bridge. So it is not difficult for him to estimate a satisfactory value of the relaxation coefficient. Normally for bridge–vehicle systems, $m > 1$ and k ranges from 0·01 to 1·0; hence, η_{max} ranges from 1·3 to 1·8 (Figure 7) and the value $p = 0{\cdot}85$ is acceptable in most cases. If the facility is available, a good relaxation coefficient can be obtained by adjusting its value to minimize the iteration number for one time step with the vehicles at a few specific positions on the bridge. Of course, a formula giving the optimum relaxation coefficient for multi-degree of freedom systems would be better but cannot be established analytically.

4. APPLICATIONS

Two examples are presented to show the performance of the proposed method. The direct time integration is performed for both examples with the Average Acceleration Method, i.e. the Newmark method with parameters $\alpha = 0{\cdot}25$ and $\delta = 0{\cdot}5$.

4.1. A simplified system with 2 DOF

The first example shown in Figure 3 has already been used in the previous section to investigate the convergence characteristics of the proposed method. No forces are applied; there is no damping in the system; the initial state is

$$x_1 = 0, \quad \dot{x}_1 = 0, \ddot{x}_1 = 20 \quad \text{and} \quad x_2 = 0{\cdot}2, \dot{x}_2 = 0, \quad \ddot{x}_2 = -20$$

A time interval $\Delta t = 0{\cdot}05$ is used. The convergence criterion is set to $\varepsilon = 1{\cdot}0 \times 10^{-8}$ for all the following iterative methods. The solution is obtained by the proposed iterative procedure with relaxation, named η-Gauss–Seidel method, with the best relaxation coefficient, i.e. calculated by equations (26) and (28): $\eta = 0{\cdot}94448$. The solution is also obtained by the proposed iteration procedure with Aitken acceleration, named Aitken-Gauss–Seidel method. The displacements, the energy of the system and the number of iterations (n_i, i.e. the last k in the Algorithm) to achieve the convergence are presented in Tables I and II for the above two methods, respectively. The system is also solved by the solution scheme (Jacobi iteration method) proposed by Hwang and Nowak[12] with the same convergence criterion as that of the proposed method to obtain the comparative results and the results are presented in Table III. To evaluate the performance of the proposed method, the solutions are also obtained with the coupled equations solved by Newmark method; these results considered as the exact values are presented in Table IV.

Table I. Results of the η-Gauss–Seidel method

t	x_1	x_2	Energy	n_i
0·00	0·000000000000000	0·200000000000000	2·000000000000000	
0·05	0·022209112676545	0·177777006628032	2·000000000000000	1
0·10	0·078916066961429	0·120979087715028	2·000000000000000	1
0·15	0·144778625239431	0·054822552389008	2·000000000000000	1
0·20	0·190321101178570	0·008636852890213	2·000000000000000	1
0·25	0·195064013529355	0·002800413954070	2·000000000000000	1
0·30	0·156646590307324	0·039663625766651	2.000000000000000	1
8·80	0·006916868350864	0·192640693903656	2.000000000000003	1
8·85	0·051146813333938	0·148994272500767	2·000000000000003	1
8·90	0·116987118707095	0·083596117199217	2·000000000000003	1
8·95	0·175135522295801	0·025602203323964	2·000000000000003	1
9·00	0·199660632101814	0·000814758984280	2·000000000000003	1

Table II. Results of the Aitken-Gauss–Seidel method

t	x_1	x_2	Energy	n_i
0·00	0·000000000000000	0·200000000000000	2·000000000000000	
0·05	0·022209112676545	0·177777006628032	2·000000000000000	2
0·10	0·078916066961429	0·120979087715028	2·000000000000000	2
0·15	0·144778625239431	0·054822552389008	2·000000000000000	2
0·20	0·190321101178570	0·008636852890213	2·000000000000000	2
0·25	0·195064013529355	0·002800413954070	2·000000000000000	2
0·30	0·156646590307324	0·039663625766651	2.000000000000000	2
8·80	0·006916868350863	0·192640693903656	2.000000000000004	2
8·85	0·051146813333937	0·148994272500766	2·000000000000004	2
8·90	0·116987118707094	0·083596117199216	2·000000000000003	2
8·95	0·175135522295801	0·025602203323964	2·000000000000003	2
9·00	0·199660632101814	0·000814758984279	2·000000000000003	2

Table III. Results of the Jacobi method

t	x_1	x_2	Energy	n_i
0·00	0·000000000000000	0·200000000000000	2·000000000000000	
0·05	0·022209087225984	0·177777021709755	1·999999189355101	6
0·10	0·078915909213266	0·120979177561010	1·999991829803469	6
0·15	0·144778159501558	0·054822798918449	1·999978529794527	6
0·20	0·190320218096949	0·008637257077043	1·999970122687484	6
0·25	0·195062814655567	0·002800800329112	1·999969690348528	6
0·30	0·156645409576104	0·039663654638985	1·999967661922030	6
8·80	0·006957440288442	0·192621813496492	1·998871709608873	6
8·85	0·051179624040226	0·148983050204729	1·998868330144712	6
8·90	0·117002132223100	0·083602440095629	1·998856504898441	6
8·95	0·175130505716195	0·025628159080296	1·998844703178712	6
9·00	0·199642239473730	0·000853605445830	1·998841360154778	6

Table IV. Results of the coupled equations

t	x_1	x_2	Energy
0·00	0·000000000000000	0·200000000000000	2·000000000000000
0·05	0·022209112676545	0·177777006628032	2·000000000000000
0·10	0·078916066961429	0·120979087715028	2·000000000000000
0·15	0·144778625239431	0·054822552389008	2·000000000000000
0·20	0·190321101178570	0·008636852890213	2·000000000000001
0·25	0·195064013529355	0·002800413954070	2·000000000000001
0·30	0·156646590307324	0·039663625766651	2.000000000000001
8·80	0·006916868350861	0·192640693903654	2.000000000000004
8·85	0·051146813333936	0·148994272500765	2·000000000000004
8·90	0·116987118707093	0·083596117199215	2·000000000000004
8·95	0·175135522295800	0·025602203323962	2·000000000000004
9·00	0·199660632101813	0·000814758984278	2·000000000000004

The comparison demonstrates the superiority of the proposed method: at the final step, results are correct up to the 15th digit while discrepancy appears in the 5th digit already with Hwang's method; the number of iterations is reduced from 6 to 1 for the relaxation method. The convergence rate is also studied on the first time step of the proposed method with relaxation, here the time step is increased to $\Delta t = 0{\cdot}15$ instead of

0·05. Different values of η are used and Figure 8 shows the number of iterations to achieve convergence versus the relaxation coefficient. The above results confirm what has been revealed in the previous section: (a) The best relaxation coefficient is much less than one in some cases; (b) The iteration converges in one iteration if the best relaxation coefficient is used or in two iterations if Aitken acceleration is effected.

All the results presented in Tables I–IV are obtained on a VAX/VMS DEC station with double precision variables of D-Float Format which has 16·85 effective digits, that is about one digit better than that of the standard IEEE double precision float.

4.2. The Yangtze-River Bridge under a moving train

The practical example of the Yangtze-River Bridge with double railway tracks built at Wuhan in China in 1957, computed by the first author in 1988,[11] is re-processed and presented here. The bridge consists of 9 spans of box girder beams with 16 m high and 10 m wide; each span is of 128 m long; every 3 spans are connected together.

The 3 spans near the left bank (Figure 9) are considered and modelled in 3D space by the Craig–Bampton[23] modal synthesis method: the whole structure is uncoupled into 3 substructures, each span

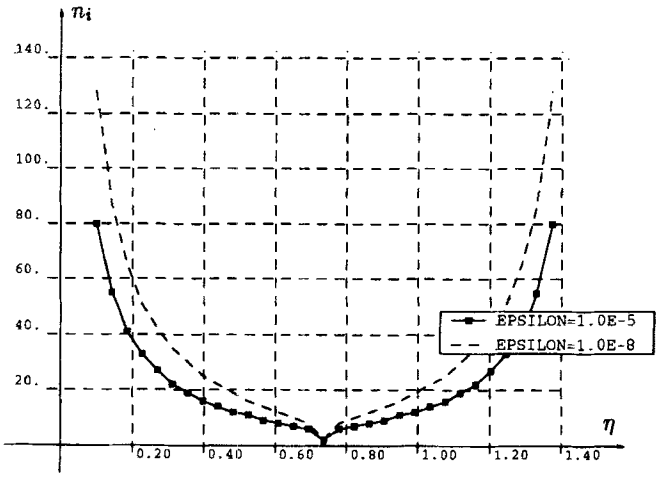

Figure 8. Iteration number n_i to achieve convergence versus relaxation coefficient η

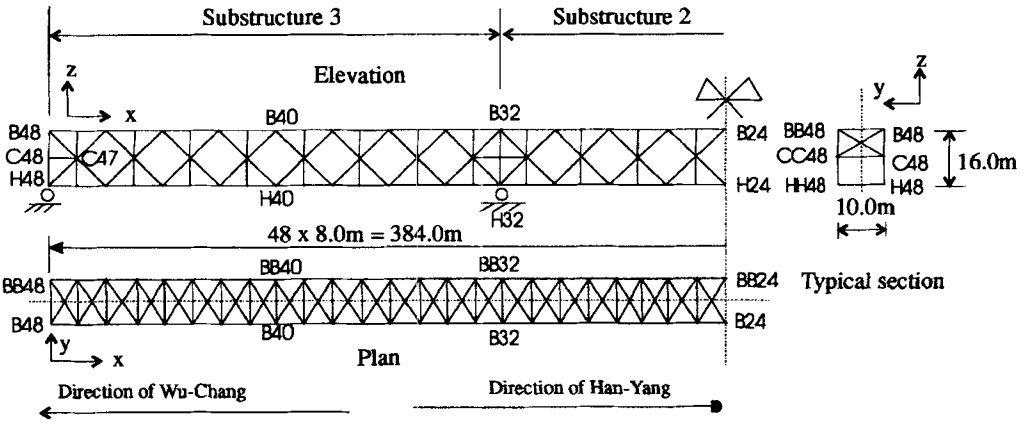

Figure 9. Yangtze-River Bridge at Wuhan

being a substructure. In addition to the constraint modes associated with the interface degrees of freedom, 24 constrained natural modes for each of the two side spans and 21 constrained modes for the central span are used to construct the dynamic model of the bridge. The effect of the highway on the top chords (B-BB plan) of the bridge is taken into account: its entire mass is added to the top chords but its stiffness reduced by 20 per cent is added to the top chords by modifying their section area. The mass of the railway facilities on the bottom chords (H-HH plan) is added to the bottom chords. This model gives the following natural frequencies of the bridge (Table V). The second and third modes can be identified as pure transverse modes (in the direction y in Figure 9) while the sixth and thirteenth are pure vertical (in the direction z) modes by means of modal shapes.

The results from the on site test[24] effected in 1967 for the natural frequencies (Table VI) are based on the individual signals of transverse and vertical displacements at midspans after crossing of an experimental train described later.

Several frequencies involve both the transverse and vertical motion (Table VI). Clearly, identified frequencies of the pure transverse and vertical modes can be compared with numerical results (Table VII). It can be concluded that the dynamic model of the bridge is suitable.

Rayleigh damping is chosen for the bridge model:

$$C_b = \alpha_1 M_b + \alpha_2 K_b$$

where M_b and K_b are the mass and stiffness matrices of the bridge. The coefficients α_1 and α_2 are computed according to the modal damping measured from the curves of free vibrations of the bridge. From the experimental data,[24] only two modal damping coefficients are identified: the modal damping $\xi = 0{\cdot}02$ for the first pure transverse mode ($f = 0{\cdot}781$) and $\xi = 0{\cdot}03$ for the first pure vertical mode ($f = 1{\cdot}757$), which give

$$\alpha_1 = 0{\cdot}008147566, \qquad \alpha_2 = 0{\cdot}000476854$$

Table V. Natural frequencies (Hz) of the bridge (numerical results)

Mode Number	1	2	3	4	5	6	7	8	9	10
Frequency	0·706	0·737	1·038	1·321	1·436	1·651	1·722	1·789	1·931	1·979
Mode number	11	12	13	14	15	16	17	18	19	20
Frequency	2·028	2·230	2·372	2·540	2·597	2·695	2·816	3·925	3·189	3·462
Mode number	21	22	23	24	25	26	27	28	29	30
Frequency	3·546	3·594	3·729	3·749	4·197	4·314	4·572	4·899	4·912	5·136

Table VI. Natural frequencies (Hz) of the bridge (experimental results)

Transverse motion	0·781	1·074		1·952	2·050		3·709	3·806
Vertical motion			1·757	1·952	2·050	2·440	3·709	3·806

Table VII. Natural frequencies (Hz) of pure transverse and vertical modes

	Pure transverse modes		Pure vertical modes	
Numerical results	0·737	1·038	1·651	2·372
Experimental results	0·781	1·074	1·757	2·440

The train (Figure 10), passing through the bridge with the constant speed of 67 km/h along the downstream line, i.e. the line near by the chords from H0 to H48, is composed of 2 locomotives (QJ + Coal) and 4 freight cars (C62). Each vehicle is modelled by a rigid body with 5 DOF (bounce, pitch, roll, yaw and lateral motion), supported by the secondary suspension springs and connected to the massless trucks (Figure 11). There is no primary suspension system, hence the trucks are connected directly to the wheels. The wheels are considered to be unsprung moving masses in view of low frequency of the response. The initial conditions for the train are obtained by assuming that the train runs on an additional segment of the railway track with known roughness before the entrance of the bridge.

The harmonic forces produced by the unbalanced weight on the driving wheels of 2 steam locomotives are a type of external excitation. The forces acting on different rails by the same wheel-axle set have a phase difference of $\pi/2$. When the locomotive travels with the speed of 67 km/h, the total force on the side of a rail for a single QJ locomotive is P_1 and P_2 on the other side. Here

$$P_1 = 71780{\cdot}5\sin(24{\cdot}8148t)\text{N}, \qquad P_2 = 71780{\cdot}5\cos(24{\cdot}8148t)\text{N}$$

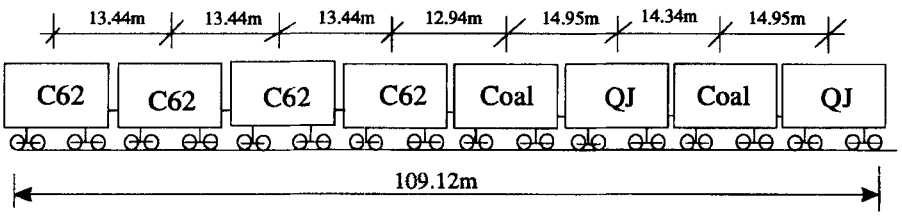

Figure 10. An example train

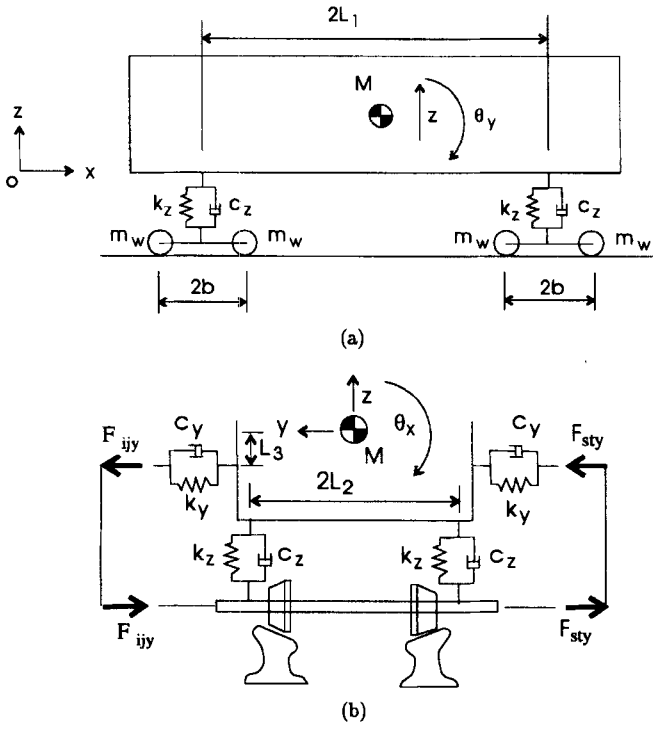

Figure 11. Vehicle model: (a) elevation; (b) side view

Supposing two locomotives produce exactly the same forces with the same phases. The hunting phenomenon is taken into account by assuming that all the wheel-axle sets move relatively to the bridge deck following a sinusoidal curve in the horizontal plan:

$$y = A_s \sin\left(\frac{x}{L_s}\right)$$

with the amplitude $A_s = 0{\cdot}005$ m and the wavelength $L_s = 17{\cdot}4$ m for the considered wheel-axle sets. With the conicity of 1·25 per cent of the wheels, a vertical relative motion of the wheels is produced because of their horizontal relative motion to the bridge deck. The hunting phenomenon is also a type of external excitation.

To find the best relaxation coefficient, the train is placed at the middle of the first span, then the relaxation coefficient is adjusted so as to minimize the number of iterations. Figure 12 shows the number of iterations to achieve convergence versus the relaxation coefficient; it can be observed that the best relaxation coefficient is near 0·95 when the train is at the assumed position. But this value is not used and the value $\eta = 0{\cdot}85$ is

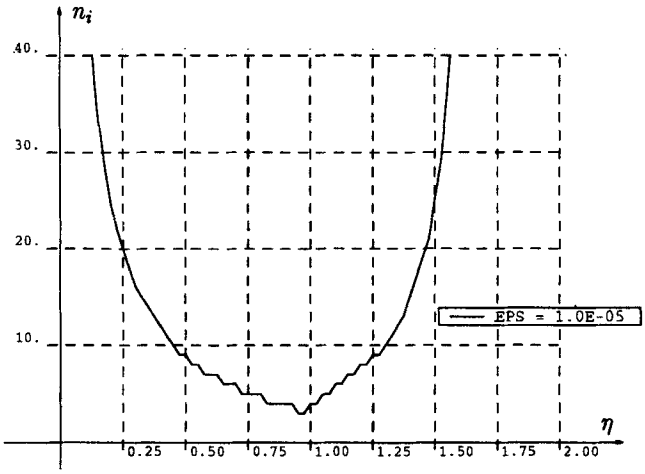

Figure 12. Iteration number n_i to achieve convergence versus relaxation coefficient η

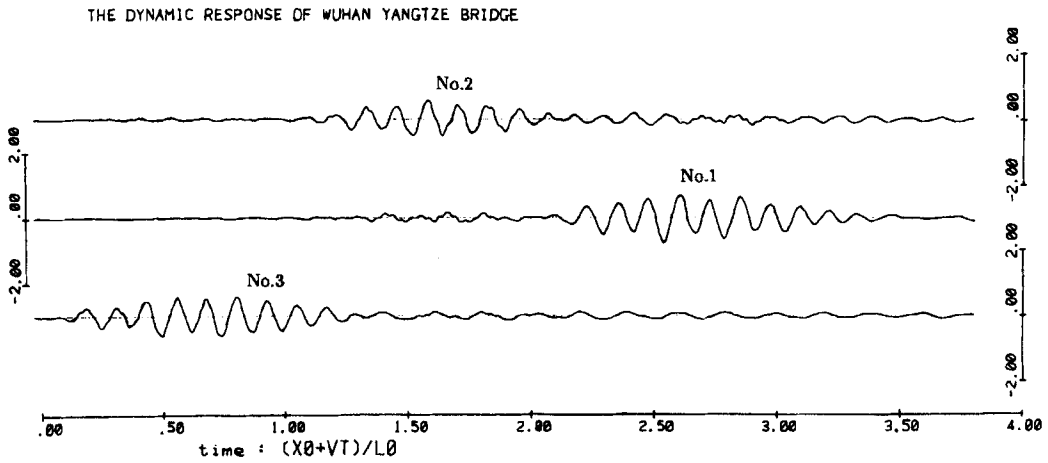

Figure 13. Transverse displacements at mid-spans of the bottom chords and downstream side: (No. 1) Node H8; (No. 2) Node H24; (No. 3) Node H40

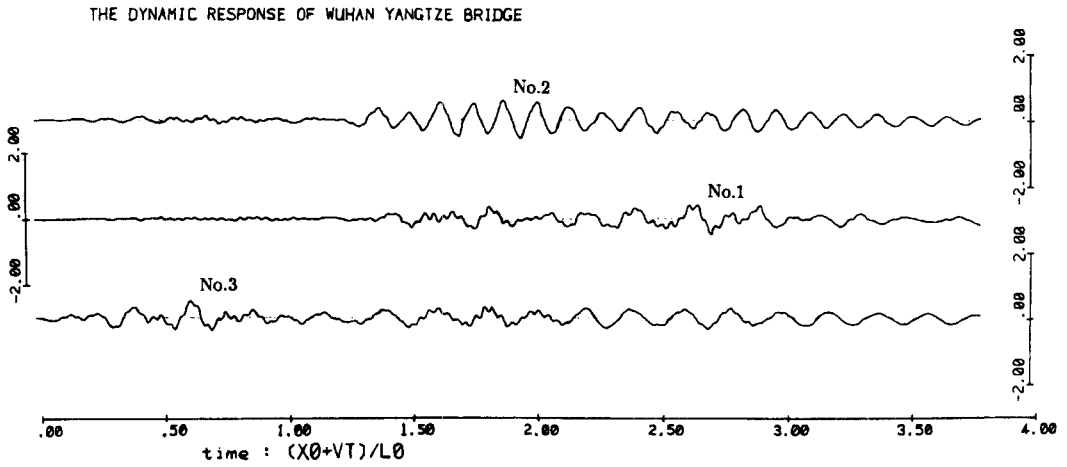

Figure 14. Transverse displacements at mid-spans of the top chords and downstream side: (No. 1) Node B8; (No. 2) Node B24; (No. 3) Node B40

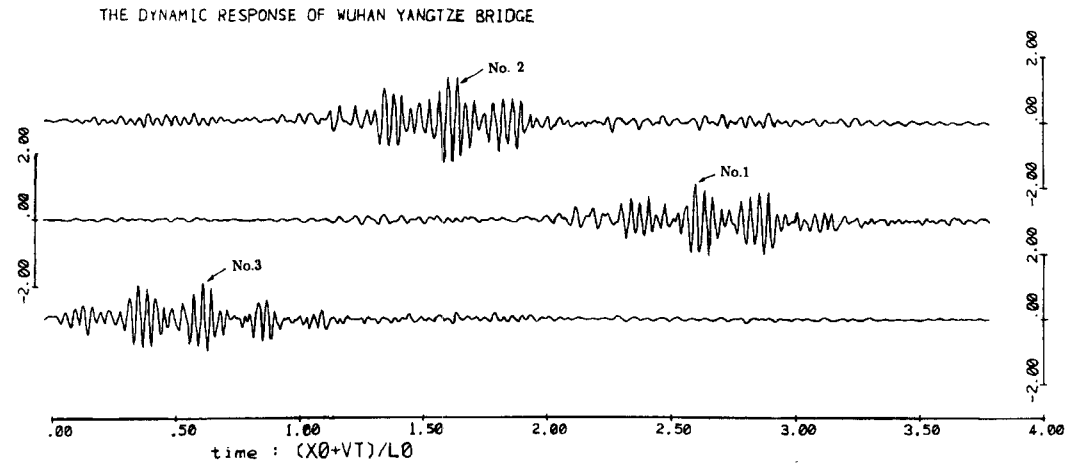

Figure 15. Vertical displacements at mid-spans of the bottom chords and downstream side: (No. 1) Node H8; (No. 2) Node H24; (No. 3) Node H40

adopted for the whole passage of the train across the bridge. Because the frequency of the dynamic response is principally below 6 Hz, the time interval of 0·04 s is proved adequate for direct time integration of the equations of motion. With the convergence criterion $\varepsilon = 1{\cdot}0 \times 10^{-5}$, the number of iterations to achieve convergence is between 4 and 6 for all time steps if the relaxation technique is used, but the iteration procedure with Aitken acceleration takes only 2 or 4 iterations to converge throughout the entire solution. It must be mentioned that, in this example, the vehicles possess unsprung masses which did not appear in the previous section; but the unsprung masses being small, they have little influence on the characteristics of iteration.

The pure numerical dynamic response computed with the proposed method, i.e. the total dynamic response from which the pseudo-static response has been subtracted, at certain points of the bridge is presented in Figures 13–16. In these figures, the maximum vertical and transverse displacements are 1·38 and 0·80 mm, respectively, and the maximum vertical acceleration is 0·11 g. The on site tests are effected in 1987, in which the first author took part, with train speeds slightly different from the computational one.

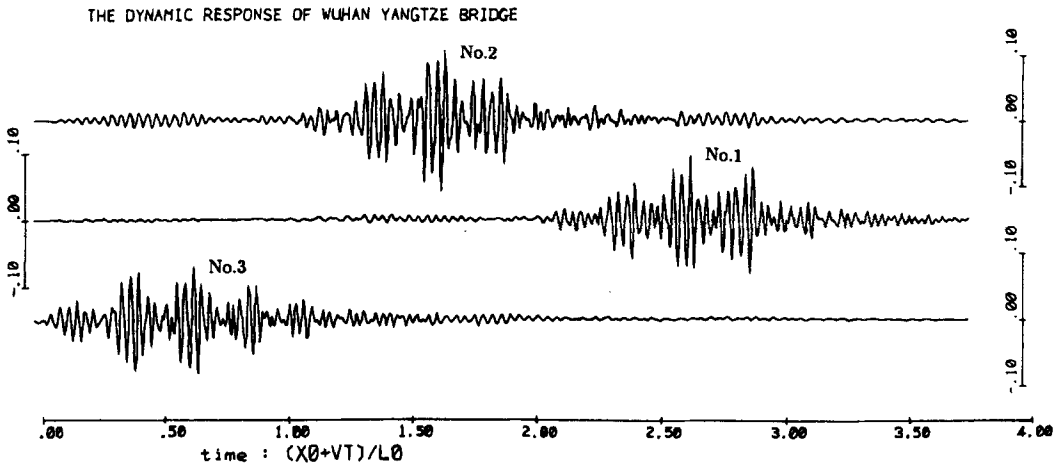

Figure 16. Vertical accelerations at mid-spans of the bottom chords and downstream side: (No. 1) Node H8; (No. 2) Node H24; (No. 3) Node H40

Table VIII. Maximum displacements (mm)

Train speed	Transverse displacement			Vertical displacement		
	Span 1	Span 2	Span 3	Span 1	Span 2	Span 3
67	0·80	0·60	0·61	1·14	1·38	1·11
65·6	0·61	0·67	0·44	0·34	0·49	0·56
65·6	0·54	0·62	0·44	0·39	0·65	0·58
66·6	0·81	0·40	0·53	0·34	0·95	0·47
67·8	0·61	0·53	0·53	0·29	1·07	0·64

Table VIII gives some of the numerical and on site test results (effected in 1987) for the maximum transverse and vertical displacements at mid-spans, bottom chords, downstream of the bridge. In this table, the results corresponding to the velocity $V = 67$ km/h are obtained by the proposed numerical method, and the others are obtained by the on-site tests. The differences between the numerical results and the site test ones can be explained. The highway deck on the top chord is taken into account by modifying the properties of the chords; only some elements are modelled with beam elements so as to maintain the structure to be statically defined and others are modelled by truss elements; the hunting phenomenon is accounted for by a simple sine curve; moreover the table clearly shows that the same train speed does not give the same results. Although many factors are not yet taken into account in the present modelisation, the above results can still give useful information about the dynamic response of the bridge.

5. CONCLUSIONS

An iterative solution method has been proposed to analyse the dynamic response of bridge–vehicle systems. The system is divided into two parts at the interface of the bridge and vehicles. The two sets of equations for these two parts are solved separately by means of the proposed iterative method with relaxation or with Aitken acceleration. If the coupling along the moving direction between the vehicles is not taken into account, the vehicles can be uncoupled and solved separately too. All these efforts make it possible to use very efficiently the computer central memory and avoid forming the coefficient matrices for the coupled equations. So one is free to pay more attention to model the two subsystems with high accuracy. The

relaxation coefficient between zero and η_{max} ensures the convergence of the iterative procedure. For the simplified system, the best relaxation coefficient is one-half of η_{max} and is always less than one. Normally one can get a good convergence rate if the relaxation coefficient is about 0·85. The iterative procedure with Aitken acceleration seems better than that with relaxation. In that case, the best relaxation coefficient is not needed but a good convergence rate can be always attained.

The first author's work completed in China Academy of Railway Sciences showed that this algorithm is very efficient for linear systems compared to the method of solving the coupled equations. This algorithm is expected to be more efficient for non-linear systems, because the iterations are necessary anyway in this case.

REFERENCES

1. S. Timoshenko and D. H. Young, *Vibration Problems in Engineering*, 3d edn., Van Nostrand Co., New York, 1955, p. 359.
2. R. K. Wen, 'Dynamic response of beams traversed by two-axle loads', *J. eng. mech. div. ASCE* **86**, No. EM5, 91–111 (1960).
3. L. S. Jacobsen and B. S. Ayre, *Engineering Vibrations*, McGraw-Hill, New York, 1958, pp. 534–536.
4. K. H. Chu, V. K. Garg and L. D. Chaman, 'Railway-bridge impact: simplified train and bridge model', *J. struct. div. ASCE* **105**, 1823–1844 (1979).
5. A. Wiriyachai, K. H. Chu and V. K. Garg, 'Impact study by various bridge models', *Earthquake eng. struct. dyn.* **10**, 31–45 (1982).
6. A. Wiriyachai, K. H. Chu and V. K. Garg, 'Bridge impact due to wheel and track irregularities', *J. eng. mech. div. ASCE* **108**, 648–666 (1982).
7. J. C. O. Nielsen and T. J. S. Abrahamsson, 'Coupling of physical and modal components for analysis of moving non-linear dynamic systems on general beam structures', *Int. j. num. methods eng.* **33**, 1843–1859 (1992).
8. A. S. Veletsos and T. Huang, 'Analysis of dynamic response of highway bridge', *J. eng. mech. div. ASCE* **96**, 593–620 (1970).
9. W. Xu, 'Space dynamic interaction between railway bridge and trains', *Ph.D. Thesis*, China Academy of Railway Sciences, 1988.
10. W. Xu, 'Calculation of the lateral wheel load of railway vehicle travelling on oscillatory bridge surface', *Proc. 4th int. conf. on computing in civil and building eng.*, Tokyo, 1991, p. 123.
11. F. H. Yang, 'Computation of dynamic responses of bridge–train system using modal synthesis method', *M. Sc. Thesis*, China Academy of Railway Sciences, 1988.
12. E. S. Hwang and A. S. Nowak, 'Simulation of dynamic load for bridges', *J. struct. eng. ASCE* **117**, 1413–1434 (1991).
13. T. L. Wang and D. Z. Huang, 'Cable-stayed bridge vibration due to road surface roughness', *J. struct. eng. ASCE* **118**, 1354–1374 (1992).
14. T. L. Wang, D. Z. Huang and M. Shahawy, 'Dynamic response of multigirder bridges', *J. struct. eng. ASCE* **118**, 2222–2238 (1992).
15. D. Z. Huang and T. L. Wang, 'Impact analysis of cable-stayed bridges', *Comput. struct.* **43**, 897–908 (1992).
16. D. Z. Huang, T. L. Wang and M. Shahawy, 'Impact analysis of continuous multigirder bridge due to moving vehicles', *J. struct. eng. ASCE* **118**, 3427–3443 (1992).
17. P. K. Chatterjee, T. K. Datta and C. S. Surana, 'Vibration of suspension bridges under vehicular movement', *J. struct. eng. ASCE* **120**, 681–703 (1994).
18. M. F. Green and D. Cebon, 'Dynamic response of highway bridges to heavy vehicle loads: theory and experimental validation', *J. sound vib.* **170**, 51–78 (1994).
19. R. Keymeulen and A. Winand, 'Modélsation mathématique simplifiée de l'interaction vehicule ferroviaire-pont et verifications expérimentales', *Annales des travaux publics de Belgique, No. 4, 97–112* (1987).
20. Ph. Van Bogaert, 'Dynamic response of trains crossing large span double-track bridges', *J. construct. steel res.* **24**, 57–74 (1993).
21. M. A. Saadeghvaziri, 'Finite element analysis of highway bridges subjected to moving loads', *Comput. struct.* **49**, 837–842 (1993).
22. A. Jennings, *Matrix Computation for Engineers and Scientistis*, Wiley, 1977, pp. 210–212.
23. R. R. Jr. Craig and M. C. C. Bampton, 'Coupling of substructures for dynamic analysis', *AIAA j.* **6**, 1313–1319 (1968).
24. 'Measurement recordings of bridge vibrations—Vol. 2: Yangtze-River Bridge', *MICAS Internal Report* (in Chinese), Mechanical Institute of China Academy of Sciences, 1970.